INTERNATIONAL JOURNAL OF CIVIL ENGINEERING & TECHNOLOGY (IJCIET)

ISSN Print: 0976-6308 ISSN Online: 0976-6316

High Quality Peer Reviewed Refereed Scientific, Engineering & Technology, Medicine and Management International Journals

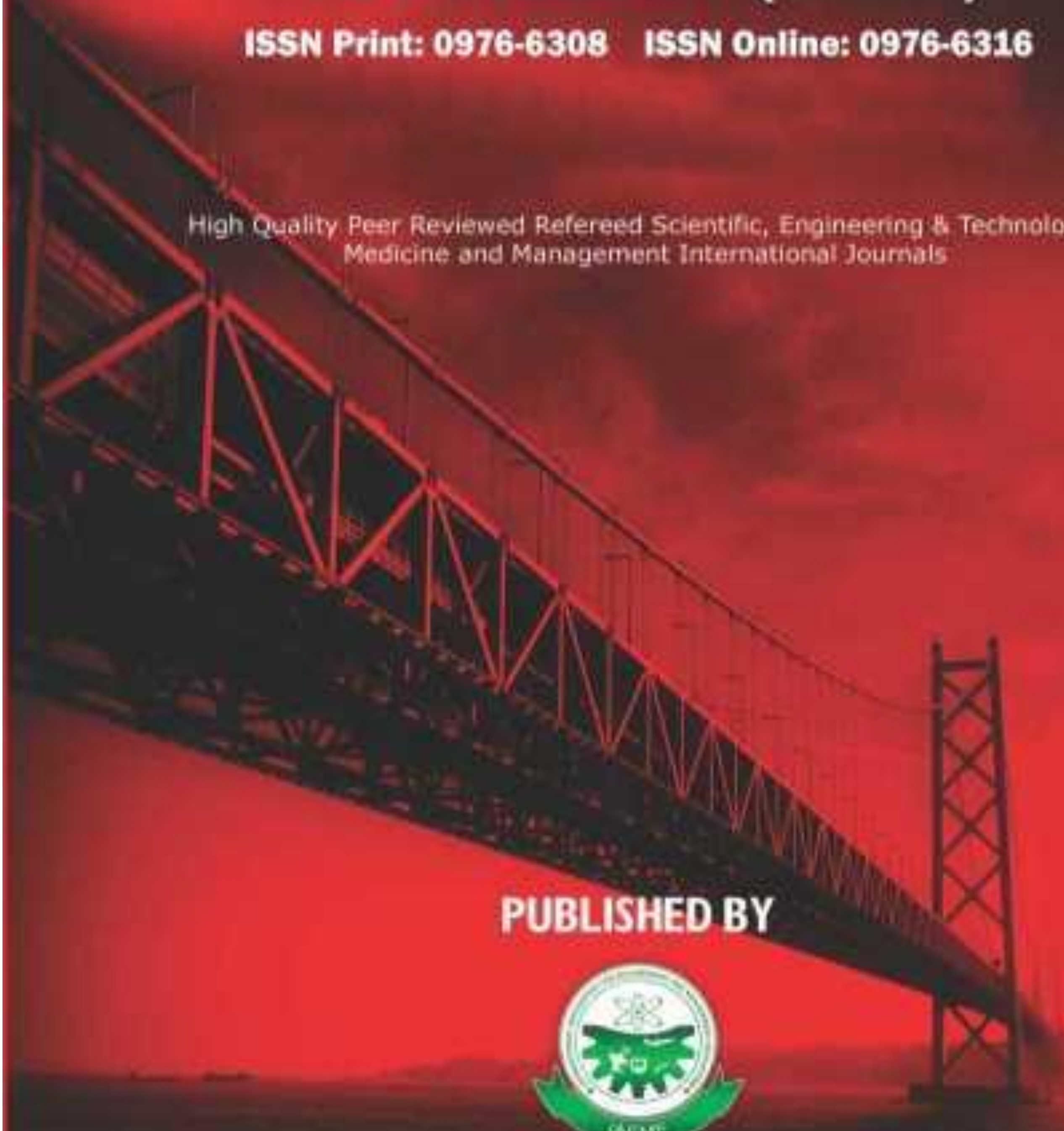

PUBLISHED BY

IAEME Publication

Plot: 03, Flat- S 1, Poomalai Santosh Pearls Apartment,
Plot No. 10, Vaiko Salai 6th Street, Jai Shankar Nagar, Palavakkam, Chennai - 600 041,
Tamilnadu, India
E-mail : editor@iaeme.com, ieamedu@gmail.com
www.iaeme.com

International Journal of Civil Engineering and Technology (IJCIET)
Volume 16, Issue 3, May-June 2025, pp. 13-42, Article ID: IJCIET_16_03_002
Available online at https://iaeme.com/Home/issue/IJCIET?Volume=16&Issue=3
ISSN Print: 0976-6308 and ISSN Online: 0976-6316
Impact Factor (2025): 21.69 (Based on Google Scholar citation)
Journal ID: 6971-8185; DOI: https://doi.org/10.34218/IJCIET_16_03_002

ASSESSING SPATIOTEMPORAL WATER QUALITY CHANGES IN THE KARNAPHULI RIVER IN BANGLADESH USING REMOTE SENSING TECHNIQUES

Kaiser Mostafiz [1]
[1] Graduate Research Assistant, Ozarks Environmental and Water Resources Institute, Missouri State University, MO 65897, United States of America.

Shishir Kumar Das [2]
[2] Graduate Teaching Assistant, Southeast Missouri State University, MO 63701, United States of America.

Mohammad Noor Uddin [3]
[3] Assistant Town Planner, Chattogram City Corporation, Bangladesh

ABSTRACT

The major rivers and lakes of Bangladesh are increasingly threatened by pollution resulting from rapid urbanization and the effects of climate change. This study assessed the water quality of the Karnaphuli River using remote sensing techniques, focusing on three key parameters—chlorophyll-a, turbidity, and surface temperature—analyzed through Landsat imagery for the years 2000, 2007, and 2015. These parameters were measured across three representative months (March, July, and November), spaced at four-month intervals, and observed at 15 georeferenced stations. The results revealed a notable decline in chlorophyll-a concentrations between 2007 and 2015 and a steady increase in turbidity levels, indicating a deterioration in water quality from moderate to severe conditions. While remote sensing proved valuable for capturing large-scale *temporal and spatial patterns, its inherent limitation in accurately detecting chemical properties such as salinity, alkalinity, and pathogens highlights the importance of integrating ground-based laboratory measurements. A hybrid approach—combining remote sensing with in-situ data collection—can enhance the accuracy of regression models and allow for the calibration and validation of satellite-derived estimates. Field surveys revealed that many river users have already reduced or ceased their use of river water and are inclined to shift to alternative sources if available, underscoring growing public concern over water safety. If current pollution trends persist, the Karnaphuli River may become unsuitable for domestic use within the next 15 years. These findings emphasize the need for continuous, integrated water quality monitoring and management strategies to safeguard river systems and support long-term water resource sustainability in the region.*

Keywords: Remote Sensing, Water Quality Assessment, Chlorophyll-a, Turbidity, Karnaphuli River, River Pollution

Cite this Article: Kaiser Mostafiz, Shishir Kumar Das, Mohammad Noor Uddin. (2025). Assessing Spatiotemporal Water Quality Changes in the Karnaphuli River in Bangladesh Using Remote Sensing Techniques. *International Journal of Civil Engineering and Technology (IJCIET)*, 16(3), 13-42.

https://iaeme.com/MasterAdmin/Journal_uploads/IJCIET/VOLUME_16_ISSUE_3/IJCIET_16_03_002.pdf

1. Introduction

Water is a fundamental resource at the heart of economic growth, public health, environmental sustainability, and social well-being (World Bank, 2016). Its availability and quality influence critical aspects of development, from food and energy security to urban resilience and poverty alleviation. However, rapid urbanization, industrialization, and climate change have intensified water quality deterioration, particularly in developing countries like Bangladesh. Rivers adjacent to major urban centers—such as the Buriganga, Shitalakhya, and Karnaphuli—are among the most affected. The Karnaphuli River, flowing beside Chittagong, the country’s second-largest city and industrial hub, has been subject to increasing pollution pressures due to unregulated discharge and encroachment. As surface water remains a primary source for domestic and industrial uses, understanding the spatial and temporal dynamics of water quality in such systems is critical for sustainable water management.

This study aims to assess water quality changes in the Karnaphuli River over a 15-year period (2000–2015) using a hybrid approach that integrates satellite remote sensing with field-based user perceptions. Specifically, it examines variations in physical water quality parameters—chlorophyll-a and turbidity—as well as surface water temperature, using Landsat imagery for the years 2000, 2007, and 2015. Additionally, surveys conducted among river water users provide insight into local awareness and behavioral responses to perceived changes in water quality. The selection of three representative months (March, July, and November) at four-month intervals allows for capturing seasonal variability across 15 georeferenced stations.

Despite the advantages of remote sensing in covering broad spatial extents and enabling long-term monitoring, it has inherent limitations in resolution and the detection of chemical parameters such as salinity, alkalinity, or microbial content. The 30-meter resolution of Landsat data restricts application to larger water bodies, and satellite-derived values may slightly differ from laboratory measurements. Nonetheless, remote sensing remains a valuable and cost-effective method, especially when complemented with field observations that allow for calibration and validation of modeled outputs. The study utilized both primary (field survey) and secondary (satellite imagery and official records) datasets to ensure robustness.

The findings from this research will inform stakeholders, including policymakers, environmental planners, and engineers, on water quality trends in urban rivers under stress. Moreover, it demonstrates the feasibility of combining geospatial techniques with community-based assessments for more informed decision-making in water resource management. As climate and urban pressures mount, such integrative monitoring frameworks will be essential for preserving aquatic health and securing sustainable access to clean water.

2. Literature Review

Water quality is a multidimensional concept encompassing the physical, chemical, and biological characteristics of water that determine its suitability for various uses (Ballance, 1996; Biswas, 2013). These characteristics are influenced by natural factors—such as topography, geology, and climate—as well as anthropogenic pressures, including urbanization, industrialization, and agricultural runoff. Rivers, in particular, exhibit complex dynamics, where discharge regimes significantly affect suspended sediment transport, nutrient fluxes, and pollutant dispersion. The Ganges River, for example, shows the highest mean annual sediment load among major rivers despite its relatively smaller basin area (UNICEF, Table 3.1).

Water quality parameters are typically categorized into three broad classes: physical (e.g., turbidity, temperature, color), chemical (e.g., pH, total dissolved solids, nutrients), and biological (e.g., bacteria, viruses, protozoa) (Aydöner, 2007). Monitoring programs—ranging from simple to advanced—are designed to evaluate these parameters, detect trends, and assess the impact of pollution or land-use changes. Remote sensing has emerged as a powerful tool for water quality assessment, particularly in large or inaccessible water bodies where traditional sampling is limited. Key parameters that can be detected via satellite sensors include chlorophyll-a, turbidity, suspended solids, and colored dissolved organic matter (CDOM) (Bhavsar, 1984; Büttner et al., 1987).

Turbidity is an optical property reflecting the scattering of light by suspended particles and is a key indicator of water clarity. High turbidity can shield pathogens from disinfectants and reduce water quality. Remote sensing quantifies turbidity by analyzing reflectance variations, particularly in red, green, and near-infrared (NIR) bands. Regression models using spectral band ratios have been shown to effectively estimate turbidity levels, with ln-transformed values producing stronger correlations (Barret, 2016).

Chlorophyll-a, a pigment found in all phytoplankton, is a widely accepted proxy for algal biomass and an indicator of eutrophication. It absorbs strongly in the blue and red portions of the spectrum while reflecting green and NIR wavelengths. Band ratio algorithms, particularly those involving the blue and red bands, have demonstrated high predictive power for chlorophyll-a estimation (Han, 1997; Jensen, 2005). For example, Luoheng Han proposed logarithmic band combinations for chlorophyll-a estimation, with the best fit involving the log ratio of blue and red bands.

Chlorophyll a measurement:

$$\text{Log (Chl-a)} = y_{\circ} + a \times \log (b_j/b_k) \quad \text{(i)}$$

$$\text{Log (Chl-a)} = y_{\circ} + a \times (b_j/b_k) \quad \text{(ii)}$$

$$\text{Log (Chl-a)} = y_{\circ} + a (\log b_j \times \log b_k) \quad \text{(iii)}$$

The best fit combination is the last one with blue and red. Hence the equation is

$$\text{Log (Chl-a)} = -9.5126 + 12.8315(\log \text{Blue} / \log \text{Red}) \quad \text{(iv)}$$

Here, Chlorophyll a is in µg / L unit.

Additional parameters relevant to water quality include CDOM, color, odor, total dissolved solids (TDS), and pH. These factors influence the optical properties of water and, in turn, affect remote sensing signals. While remote sensing is limited in detecting certain chemical or microbial constituents, it remains effective for large-scale monitoring of optical parameters, especially when integrated with ground-based measurements for calibration.

Remote sensing operates on the principle of detecting solar radiation reflected or backscattered from the water surface. The interaction of light with water depends on absorption and scattering processes, which vary with wavelength and constituent concentration. In natural waters, only 1–3% of incident solar radiation is typically backscattered to the surface, and this fraction carries the spectral signature used for remote sensing analysis (Moore, 1980; Shafique). Turbid waters scatter more light, while colored or organic-rich waters absorb more, especially in the shorter wavelengths.

The integration of remote sensing into water quality assessment provides critical advantages for monitoring spatiotemporal variability, detecting trends, and supporting management decisions. It enables efficient observation of large and dynamic systems like rivers and lakes without requiring physical access. As pollution threats continue to rise, particularly in developing regions, remote sensing offers a scalable and cost-effective method for supporting long-term environmental monitoring and policy development.

3. Materials and Methods

3.1 Study Area

The Karnaphuli River, the largest and most significant river in southeastern Bangladesh, flows through the Chittagong Hill Tracts and the city of Chittagong before draining into the Bay of Bengal. Originating in the Lushai Hills of Mizoram, India, the river stretches approximately 270 kilometers and plays a critical role in the region's hydrology, economy, and transportation. Its mouth is home to the Port of Chittagong—the country's principal seaport—underscoring its national importance for trade and commerce.

Hydrologically, the Karnaphuli is classified as an antecedent river, maintaining its course through tectonically uplifted hill ranges such as Barkal, Sitapahar, and Patiya. Major tributaries include the Kasalong, Chengi, and Halda rivers. The river's upper stretches are narrow and meandering, while downstream it widens and receives contributions from urban canals, including the highly polluted Chaktai canal. The basin's topography is largely hilly, particularly in the upstream near Kaptai and even in parts of downstream areas surrounding the Chattogram City Corporation (CCC).

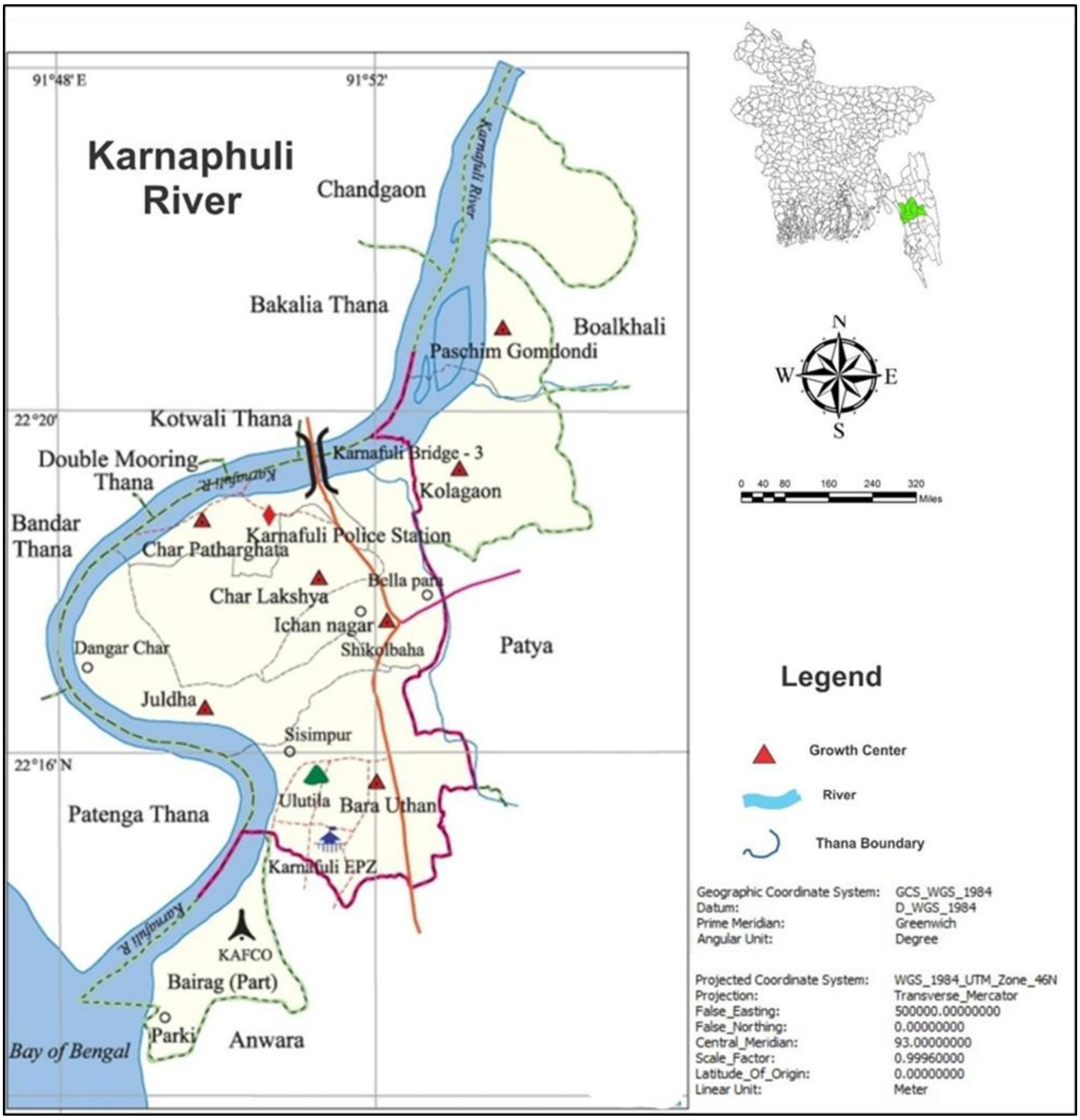

Figure 1 Geographic location of Karnaphuli river

The Karnaphuli basin lies within a tropical monsoon climate zone, characterized by high temperatures and significant seasonal rainfall. The region experiences three distinct seasons: pre-monsoon (March–May), monsoon (June–October), and post-monsoon (November–February). Rainfall is highly seasonal, with over 80% of annual precipitation—averaging 2,612 mm—occurring between June and September.

Economically, the river supports diverse activities including hydroelectric power generation, industrial production, and trade. The Kaptai Dam, constructed in 1962, created the

Kaptai Lake and remains the country's sole source of hydroelectricity. Numerous industrial facilities—including the Karnaphuli Paper Mill (KPM), the Chittagong Urea Fertilizer Limited (CUFL), and the Chittagong Export Processing Zone—have been established along the riverbanks, leveraging its logistical advantages. However, industrial growth has significantly degraded the river's ecological health. Effluent discharge from factories and untreated urban runoff, particularly via the Chaktai canal, have contributed to severe pollution, especially in the downstream sections.

This degradation threatens the river's rich biodiversity. Once home to abundant species such as the Ganges river dolphin and various commercially important fish like Hilsha, recent years have witnessed a decline in aquatic life due to habitat disruption and contamination. Historically, the Karnaphuli has served as a crucial node in regional maritime trade, attracting merchants from Arabia, Persia, China, and Europe since the medieval period. Sites such as Firingi Bazaar and accounts from the liberation war further underscore its cultural and historical importance.

The Karnaphuli River thus represents a complex socio-environmental system, balancing vital economic functions with increasing environmental vulnerabilities. Understanding its spatiotemporal water quality dynamics is essential for formulating sustainable management strategies in the face of rapid urban-industrial expansion.

3.2. Methodology

This study employed an integrated approach combining remote sensing analysis with primary field surveys to assess changes in water quality in the Karnaphuli River, Chittagong, over a 15-year period. The research was motivated by growing concerns over the impacts of climate variability and urbanization on riverine systems. The Karnaphuli River was selected as the study area due to its ecological and economic importance, as well as its vulnerability to environmental stressors.

Three key water quality parameters—chlorophyll-a, turbidity, and surface temperature—were selected to meet the study's objectives. The methodological framework included literature review, satellite image analysis, and household-level surveys of river water users. Relevant scientific literature from journals such as Elsevier, JSTOR, and the International Journal of Remote Sensing informed the selection of remote sensing techniques. In particular, previous work by Professor Han (University of Alabama) on water quality estimation using satellite-derived band ratios guided the remote analysis procedures. Landsat imagery (Landsat 7 and 8) from the USGS Earth Explorer platform was used to extract water quality data for the years 2000, 2007, and 2015, for the months of March, July, and November—capturing seasonal variations. Due to cloud cover, July 2015 imagery was excluded. Four spectral bands—Blue, Green, Red, and Near-Infrared (NIR)—were used to estimate chlorophyll-a and turbidity values using ERDAS Imagine 2014 and ArcGIS 10.3 software.

Primary data were collected via household surveys conducted in upstream riverine communities. A reconnaissance visit was first carried out to identify active river water users. The downstream region had minimal direct usage, whereas the upstream area, particularly near Betagi (Raozan) and Sitapahar (near Lichubagan), had more residents dependent on river water for daily needs. Two clusters were selected for survey: 28 respondents in Betagi and 25 in Sitapahar.

A standard sampling formula, following Sufian (1998), was used to determine the sample size at a 95% confidence level and ±0.4 error tolerance. The calculated crude sample size (n_0) was 216, adjusted using the finite population correction formula based on an estimated population of 71 households. This resulted in a final sample size of 53 respondents.

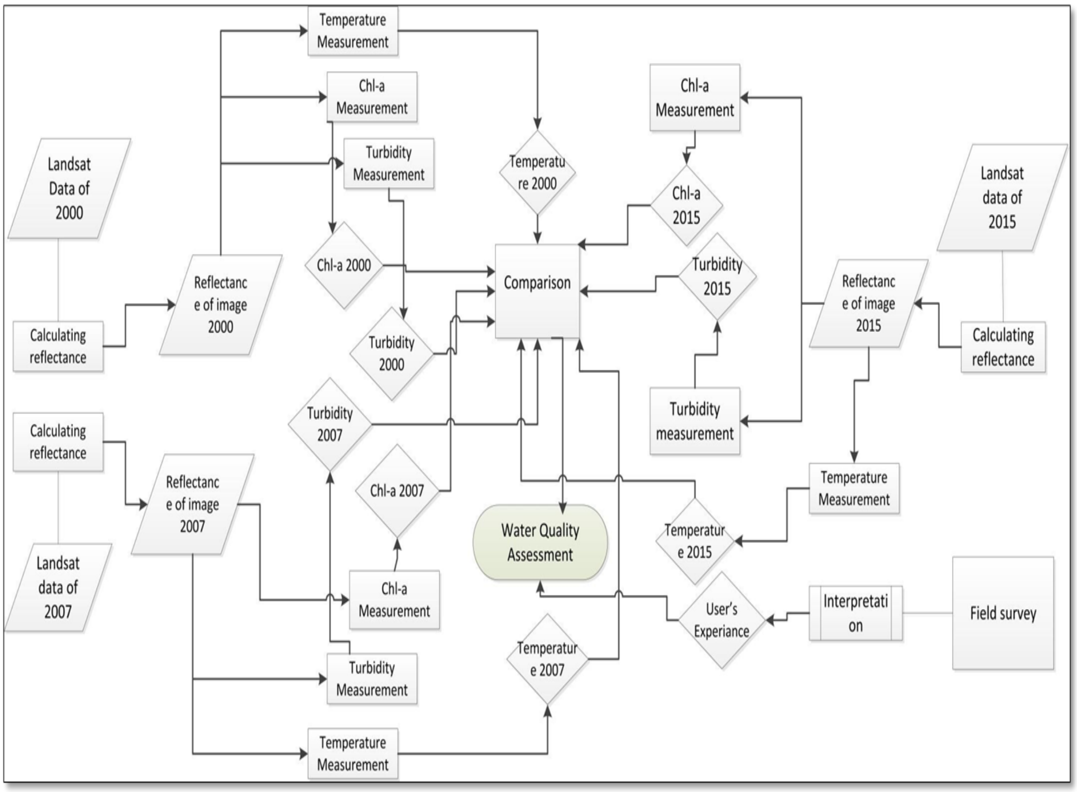

Figure 2: Work procedure of the study

Parameter Selection and Derivation:

Three water quality indicators—chlorophyll-a, turbidity, and surface temperature—were selected for analysis. These parameters are reflective of both chemical and physical conditions in surface water and are widely used in environmental monitoring. (1) Chlorophyll-a was estimated using the log ratio of blue and red bands from Landsat imagery, applying a regression model developed by Han (1994). (2) Turbidity was derived using a multi-band regression equation incorporating Red, NIR, Green, and Blue reflectance values. The final turbidity values were expressed in NTU (Nephelometric Turbidity Units) after anti-log transformation. (3) Surface Temperature was calculated from thermal bands using sensor-specific equations. ETM+ and TM data were processed using a two-step DN-to-radiance and radiance-to-temperature conversion, while Landsat 8 followed a separate calibration protocol. Final temperatures were converted from Kelvin to degrees Celsius.

3.2.1. Secondary Data

This study utilized secondary data derived from multi-temporal Landsat satellite imagery with a spatial resolution of 30 × 30 meters, which is suitable for monitoring large-scale environmental changes in river systems. The imagery was acquired from the United States Geological Survey (USGS) Earth Explorer platform and spans three distinct years—2000, 2007, and 2015—each representing different seasonal conditions through the selection of three months: March, July/August, and November.

The characteristics of the acquired Landsat images, including acquisition dates, cloud cover percentages, sensor types, and scene IDs, are presented in the tables below.

Table 1: Characteristics of Acquired Landsat Images for the Year 2000

Month	Acquisition Date	Cloud cover (%)	Sensor	Landsat scene ID
March	2000- 03- 27	17	ETM+	"LE71360452001086SGS00"
July	2000- 07- 30	50	ETM+	"LE71360452000212SGS00"
November	2000- 11- 03	5	ETM+	"LE71360452000308SGS00"

Table 2: Characteristics of Acquired Landsat Images for the Year 2007

Month	Acquisition Date	Cloud cover	Sensor	Landsat scene ID
March	2007- 03- 20	1	TM	"LT51360452007079BKT00"
July	2007- 07- 24	33	TM	"LT51360452007175BKT00"
November	2007- 11- 01	0	TM	"LT51360452008306BJC00"

Table 3: Characteristics of Acquired Landsat Images for the Year 2015

Month	Acquisition Date	Cloud cover	Sensor	Landsat scene ID
March	2015- 03- 26	0.73	OLI_TIRS	"LC81360442015085LGN00"
August	2015- 08- 18	46.9	OLI_TIRS	"LC81360452015261LGN00"
November	2015- 11- 21	0.2	OLI_TIRS	"LC81360452015325LGN00"

The selection of these images prioritized low cloud coverage to ensure better visibility of water bodies for analysis. The bands used in this study—Blue, Green, Red, and Near-Infrared (NIR)—were consistent across years to maintain comparability in water quality assessment.

3.2.1. Surface Reflectance Calculation

Surface reflectance was calculated for each selected month and year using band-specific metadata and sensor-specific algorithms. Landsat 7 ETM+ and TM methodologies were used for the years 2000 and 2007, while Landsat 8 OLI_TIRS methods were applied for the 2015 images. Prior to reflectance computation, the Karnaphuli River study area was subset from the raw imagery using ArcGIS and ERDAS Imagine software.

Landsat 7 ETM+ and TM (2000 & 2007):

A two-step process was followed: converting digital number (DN) values to radiance, and then from radiance to surface reflectance.

Radiance Calculation Example (Band 1, November 2000):

$$\text{Radiance}= ((191.6-(-6.2) / (255\text{-}1)) \times(\text{DN}-1) +(-6.2)$$

Where:

- Lmaxλ> = 191.6, Lminλ = -6.2, Qcalmax= 255, Qcalmin= 1.

  Reflectance = (3.1416 ×Rad × 1.00783572) / (1969 ×sin 38.93538338)

Where:

- 1.0078 = Earth-sun distance (AU),
- 1969 = Mean solar exo-atmospheric irradiance for Band 1,
- 38.9353° = Sun elevation angle (metadata).

Landsat 8 OLI_TIRS (2015)

Landsat 8 surface reflectance was calculated using a one-step TOA reflectance conversion:

$$P\lambda = M\rho \times Qcal + A\rho$$

Where:

- Mρ=2.0000×10−5M_{\rho} = 2.0000 \times 10^{-5}Mρ=2.0000×10−5,
- Aρ=−0.1A_{\rho} = -0.1Aρ=−0.1,
- Q_{cal} = DN value.

Final reflectance was derived as:

$$P\lambda = P\lambda' / Sin\theta$$

Where, θ = Sun elevation angle (From image metadata)

4.8 Water Quality Parameter Selection and Estimation

Three key parameters—Chlorophyll-a, Turbidity, and Surface Temperature—were selected for assessing river water quality. These indicators reflect both physical and chemical characteristics relevant to ecosystem health and usability.

Chlorophyll-a Estimation

Chlorophyll-a was estimated using band ratios from the Landsat ETM+ sensor (Blue and Red bands). The logarithmic regression model used is:

$$\log(\text{Chl-a}) = -9.5126 + 12.8315(\log(\text{Red}) / \log(\text{Blue}))$$

After computing log values, anti-log transformation was applied to obtain Chl-a in µg/L.

Example Calculation:

- log(Blue) = -0.8735
- log(Red) = -0.8189

$$\log(\text{Chl-a}) = -9.5126 + 12.8315 \times (0.8735 / 0.8189) = 4.1744$$

$$\text{Chl-a} = \text{Anti log } (4.174436) = 14,942\ \mu g/L$$

Turbidity Estimation

Turbidity was calculated using band combinations of Red, NIR, Green, and Blue. The following equation was applied:

$$\ln(\text{Turbidity}) = 6.7 + 0.62(\text{Red}) - 0.882(\text{NIR}) - 3.22(\text{Green}) * (\text{NIR} / \text{Blue} + \text{Green} / \text{Blue})$$

Surface Temperature Estimation

TM and ETM+ (2000 & 2007)

Radiance Calculation:

$$L\lambda = (LMAX - LMIN) / (QCALMAX - QCALMIN) \times (QCAL - QCALMIN) + LMIN$$

Table 4: Thermal Constants for TM and ETM+

Satellite	Sensor	K1($^{-}$ep^{2-}sr^{1-}mp^{1})	K2 (Kelvin)
Landsat 7	ETM+	666.09	1282.71
Landsat 5	TM	607.76	1260.56

This methodological framework integrates geospatial technologies with field-based validation to assess water quality changes over time and space. The use of remote sensing allowed for the efficient monitoring of a large and dynamic river system, while primary data collection captured localized perceptions of environmental change. The systematic sampling of 15 river stations, combined with three temporal snapshots per year, enhances the robustness of the study and provides a replicable model for water quality assessment in similar urban-industrial river basins.

4. Analysis and Discussion

4.1 Chlorophyll-a Dynamics

This section presents the spatiotemporal variation of Chlorophyll-a concentrations in the Karnaphuli River across three reference years—2000, 2007, and 2015—using satellite-derived estimates. Chlorophyll-a, a proxy for algal biomass and a key indicator of nutrient enrichment, was analyzed for the months of March, July, and November at 15 georeferenced stations distributed at 3 km intervals along the river. The analysis reveals inter-annual fluctuations and intra-seasonal variability, reflecting the changing trophic conditions of the river.

March Observations:

In March, Chlorophyll-a concentrations in 2000 were generally low (0–100 µg/L), with two isolated hotspots near Shah Amanat Bridge and Kalurghat Bridge exceeding 500 µg/L. In 2007, average concentration increased substantially, particularly in downstream and midstream sections, marking the highest observed levels across the time series. By 2015, values had significantly declined, with low to moderate concentrations dominating the river profile. At Station 3, for example, Chlorophyll-a values dropped from 997.3 µg/L in 2000 to 88.98 µg/L in 2015, illustrating a clear downward trend.

July Observations:

The July imagery revealed a different pattern. In 2007, the river experienced widespread eutrophication, with nearly two-thirds of the river area—especially upstream—exhibiting very high Chlorophyll-a values. Station 9 recorded the peak concentration of 930 µg/L during this period. In contrast, the years 2000 and 2015 were characterized by more moderate levels, with 2015 showing a localized anomaly at Station 11, where Chlorophyll-a spiked to 783.10 µg/L. This may reflect episodic nutrient loading or stagnation in that particular reach.

November Observations:

For November, the highest average Chlorophyll-a concentrations were recorded in 2000, particularly in downstream and middle reaches. By 2007, elevated values were limited to the downstream region, while 2015 exhibited consistently low concentrations throughout the river. Stations 3, 7, and 9 showed a declining trend across the three years. However, exceptions were noted at Stations 4 and 5, where 2007 values exceeded 600 µg/L, likely due to localized algal blooms or pollution inputs.

Overall Trends:

The temporal analysis indicates that Chlorophyll-a concentrations peaked in 2007, suggesting heightened nutrient enrichment and possible eutrophication during that period. By 2015, a notable decline was observed across all seasons and most stations, potentially reflecting improved wastewater regulation, hydrological shifts, or reduced nutrient inputs. The results underscore the dynamic nature of algal productivity in the Karnaphuli River and the efficacy of satellite-based monitoring for detecting long-term changes in aquatic ecosystems.

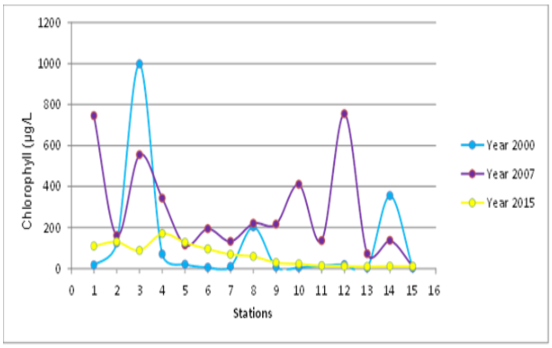

Figure 2: Chlorophyll-a at different stations in March

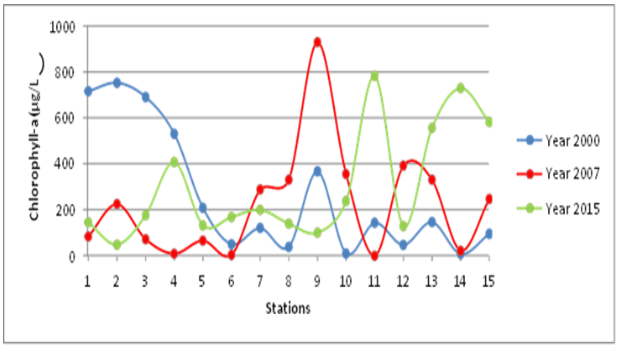

Figure 3: Chlorophyll-a at different stations for the month of July

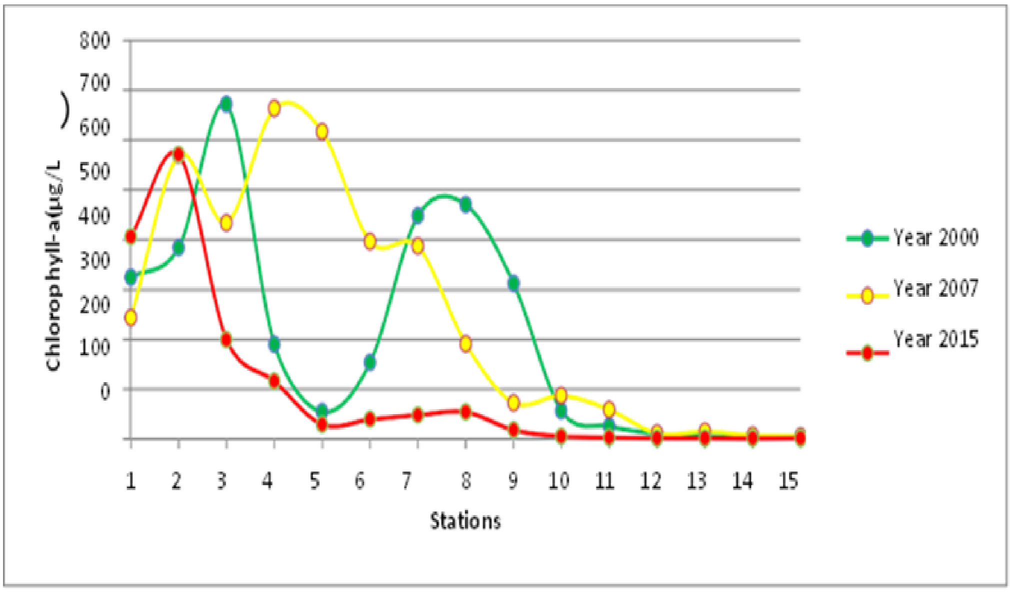

Figure 4: Chlorophyll-a at different stations for the month of July

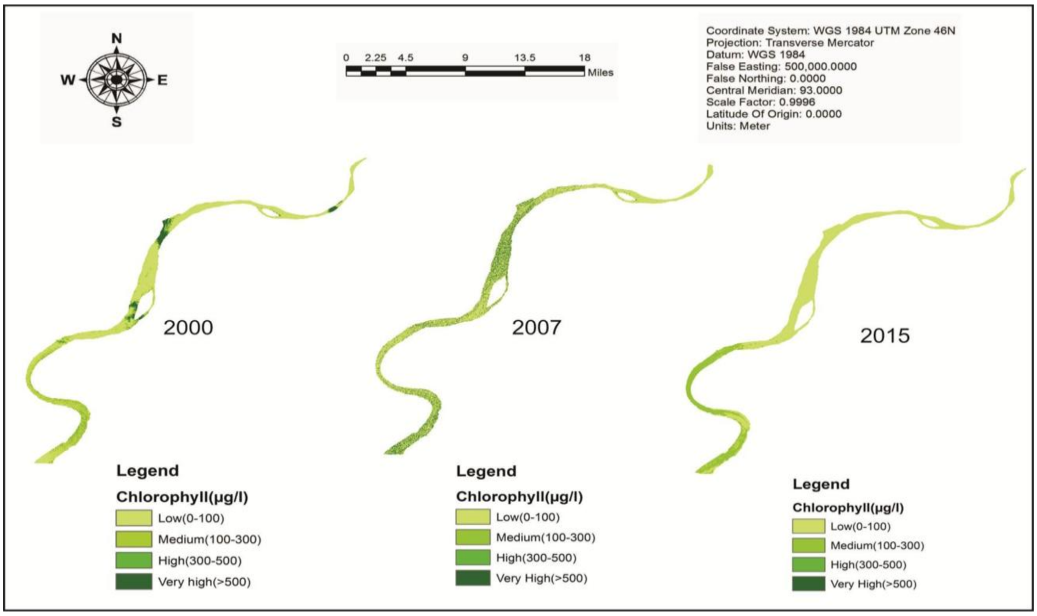

Figure 5: Chlorophyll-a for the month of March for three different stations

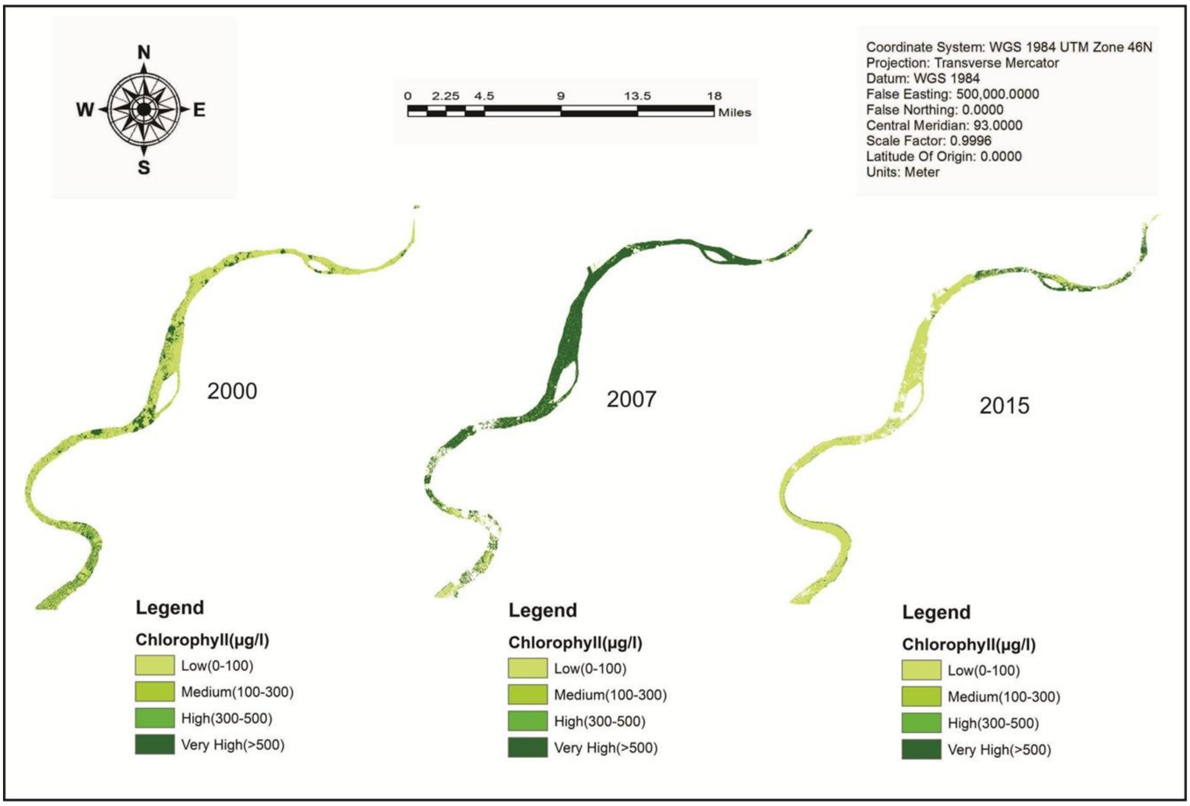

Figure 6: Chlorophyll-a for the month of July

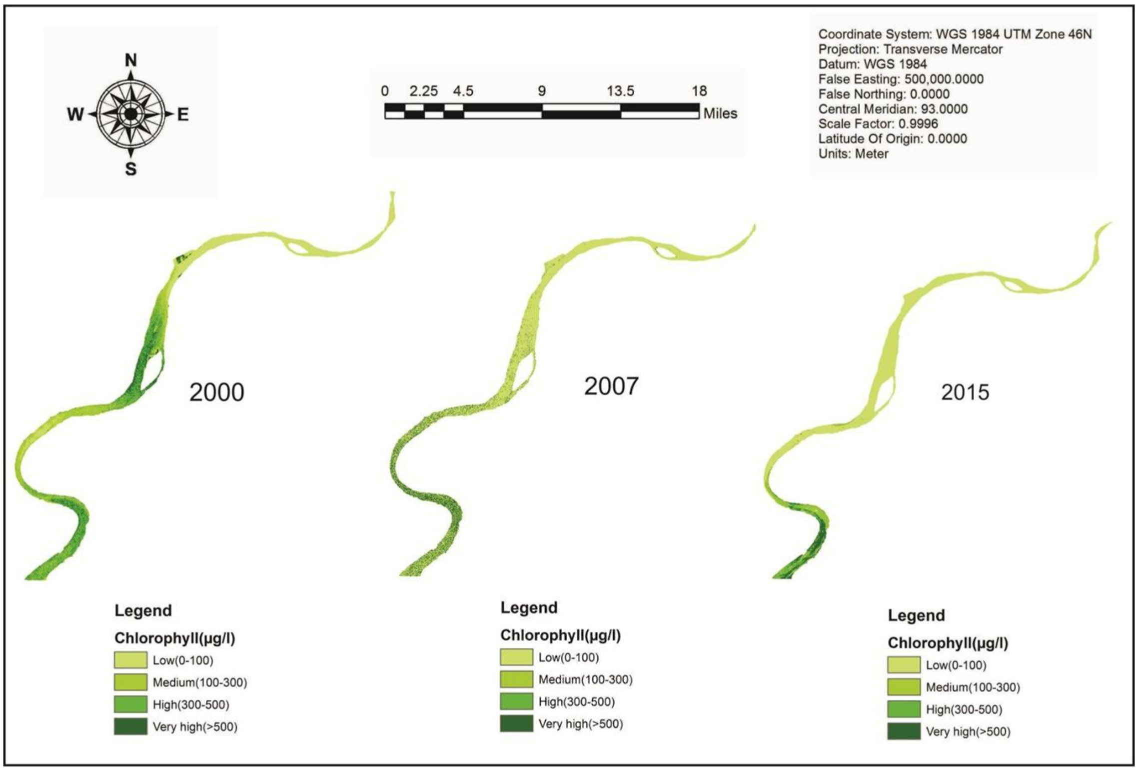

Figure 7: Chlorophyll-a for the month of November

4.2 Turbidity Analysis

Turbidity, a key indicator of water quality, was analyzed using satellite-derived imagery across three time points: 2000, 2007, and 2015. The observed values ranged from nearly 0 Nephelometric Turbidity Units (NTU) to over 200 NTU, demonstrating clear temporal and spatial variations. The monthly analysis provides insight into seasonal trends and potential anthropogenic or natural drivers influencing turbidity dynamics in the Karnaphuli River.

4.2.1 Turbidity in March

As illustrated in Figure 8, turbidity levels in March 2000 were predominantly low (0–50 NTU) throughout the river corridor, although data gaps existed in sections of the midstream reach. A similar pattern of low turbidity was observed in 2007. In contrast, the 2015 data indicated a marked increase, with medium-range turbidity (50–100 NTU) dominating the river. The downstream and some midstream portions retained low turbidity levels, but the overall trend suggests a distinct upward shift in turbidity by 2015.

Graphical comparisons of turbidity across the 15 sampling stations show that 2015 consistently reported higher average values than either 2000 or 2007. Notably, 2015 values did not overlap with those of earlier years at any station, reinforcing the inference of a significant increase in suspended particulate matter during that period.

4.2.2 Turbidity in July

Figure 9 presents the spatial distribution of turbidity for the month of July. In 2000 and 2007, the river predominantly exhibited low turbidity values, though some data were missing. However, in 2015, turbidity levels escalated dramatically, with most areas exceeding 200 NTU.

The accompanying station-wise graph further confirms this surge. Stations 6, 11, 12, and 14 recorded exceptionally high turbidity in 2015, surpassing 800 NTU. For instance, Station 6 reached 910.32 NTU, compared to 476.22 NTU in 2007 and only 45.92 NTU in 2000. While certain stations—such as 3, 9, and 13—showed minimal change over the years, the overall trend clearly highlights July 2015 as the peak period for turbidity within the study period.

4.2.3 Turbidity in November

Turbidity values in November across the three years are visualized in Figure 10 Both 2000 and 2007 maintained low turbidity levels (0–50 NTU), despite missing data in the downstream segment for 2007. In 2015, turbidity remained within a similar range but with marginal increases in the upstream stretch (Stations 8 to 15).

For example, turbidity at Station 8 in 2015 was 24.30 NTU, rising from 14.99 NTU in 2007 and 0.17 NTU in 2000. Though this increasing pattern persisted upstream, none of the values surpassed the 50 NTU threshold, thereby classifying all three years within the same visual category on the map. The midstream and downstream stations exhibited more irregular trends with no clear pattern of change.

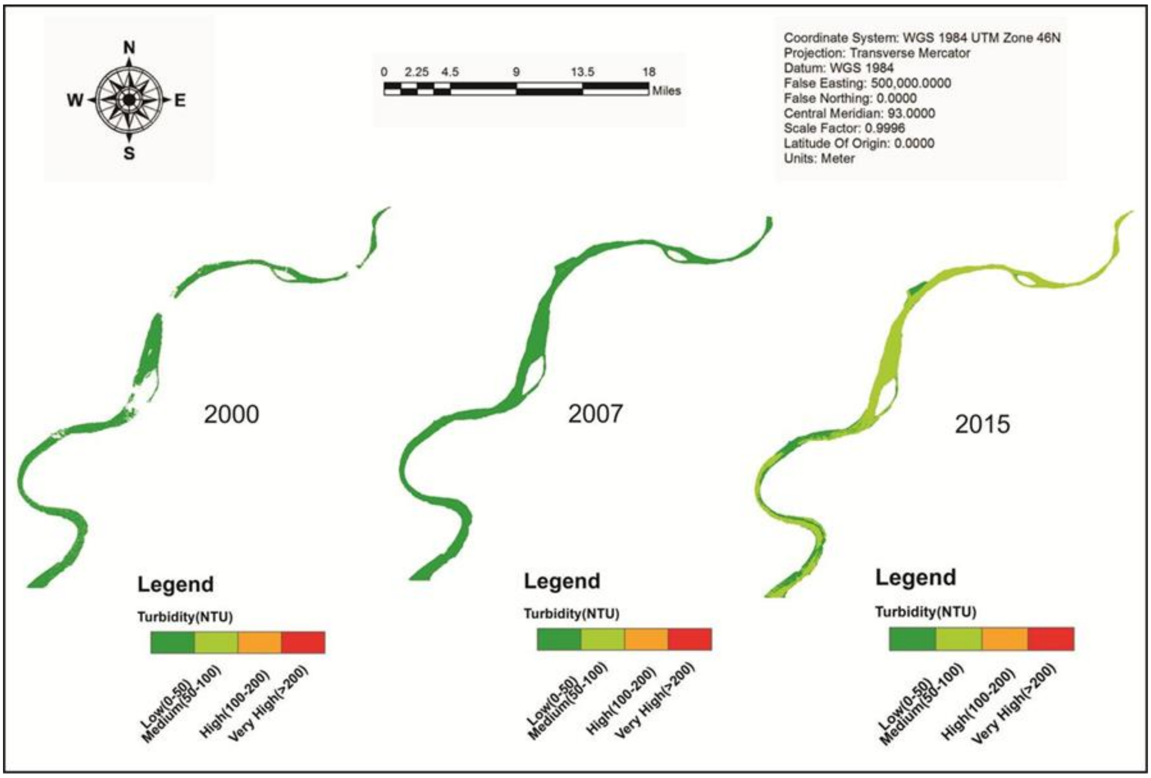

Figure 8: Turbidity for the month of March

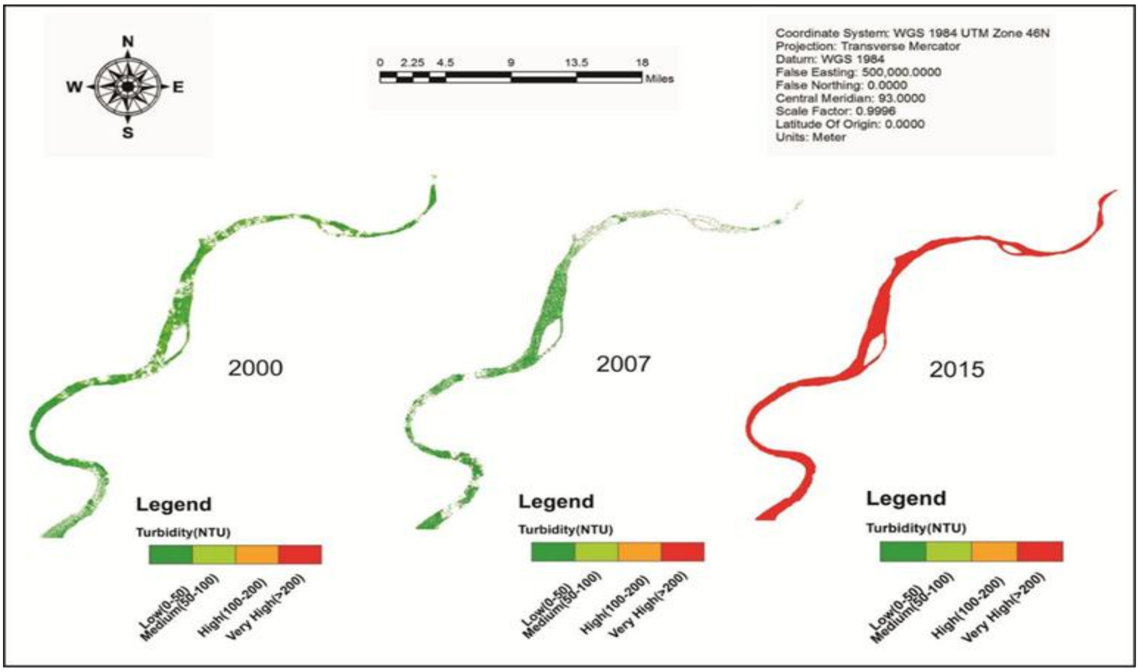

Figure 9: Turbidity for the month of July

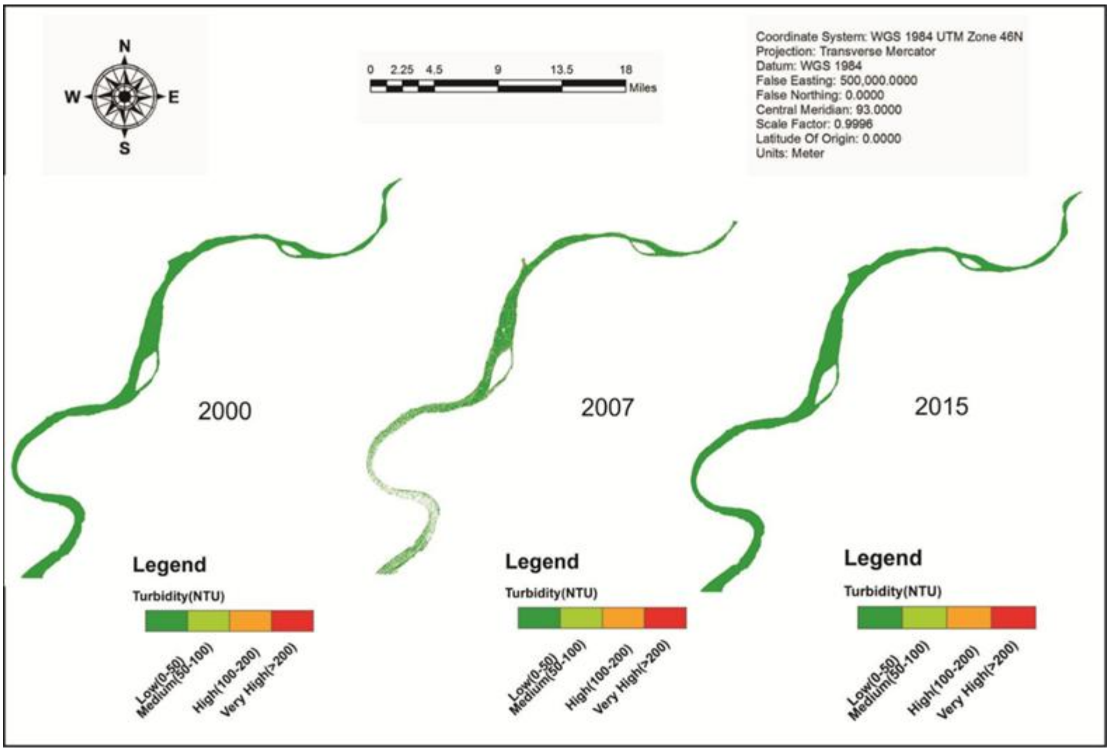

Figure 10: Turbidity in Novemver

4.3 Temperature Analysis

Surface water temperature is a crucial parameter for assessing riverine ecological conditions and biogeochemical processes. In this study, satellite-derived temperature data were categorized into four classes to facilitate comparison: Very High (24–28°C), High (21–24°C), Medium (19–21°C), and Low (<19°C). The spatial and temporal variations of temperature across three selected years—2000, 2007, and 2015—were analyzed for the months of March, July, and November.

4.3.1 Temperature in March

As illustrated in Figure 11, the temperature distribution in March 2000 was predominantly within the high range (21–24°C), with some isolated regions exhibiting medium or low values. In 2007, temperature values increased noticeably, with many areas—particularly the middle and downstream sections—reaching the very high category (24–28°C), especially near the riverbanks. The 2015 temperature pattern resembled that of 2000 but exhibited localized regions of very high temperatures.

The corresponding station-wise graph confirms that, despite minimal year-to-year variation, 2007 consistently recorded the highest average temperatures for March. The 2007 temperature trend line remained above those of both 2000 and 2015 across all 15 stations, indicating a warmer river environment during that year.

4.3.2 Temperature in July

Figure 12 displays the July temperature profiles for all three years. In 2000 and 2015, the Karnaphuli River exhibited predominantly low temperature values, while in 2007, the entire river was characterized by medium to high temperature ranges. The spatial maps suggest a pronounced warming pattern in 2007, consistent across all river segments.

Graphical data from the 15 monitoring stations further validate this finding. The 2007 temperature line remained consistently higher, notably peaking at Station 10, where the temperature reached 20.91°C, compared to 15.53°C in 2000 and only 7.12°C in 2015. A similar descending pattern—2007 > 2000 > 2015—was evident across Stations 8 to 12, reinforcing the year's status as the warmest July within the study period.

4.3.3 Temperature in November

Figure 13 presents the spatial temperature distribution for November. Across all three years, the river experienced high to very high temperatures. In 2000, temperatures predominantly fell within the high category, whereas both 2007 and 2015 exhibited widespread very high temperatures.

The station-wise analysis highlights that 2000 recorded the lowest average temperatures, consistently below the levels of 2007 and 2015. The 2000 temperature curve remained distinct and lower, with all recorded values still above 23°C. In contrast, the 2015 data revealed the highest temperature values, particularly across Stations 1 through 6, where values approached 26°C, most notably at Stations 2 and 6. These findings indicate a clear warming trend during November over the 15-year period.

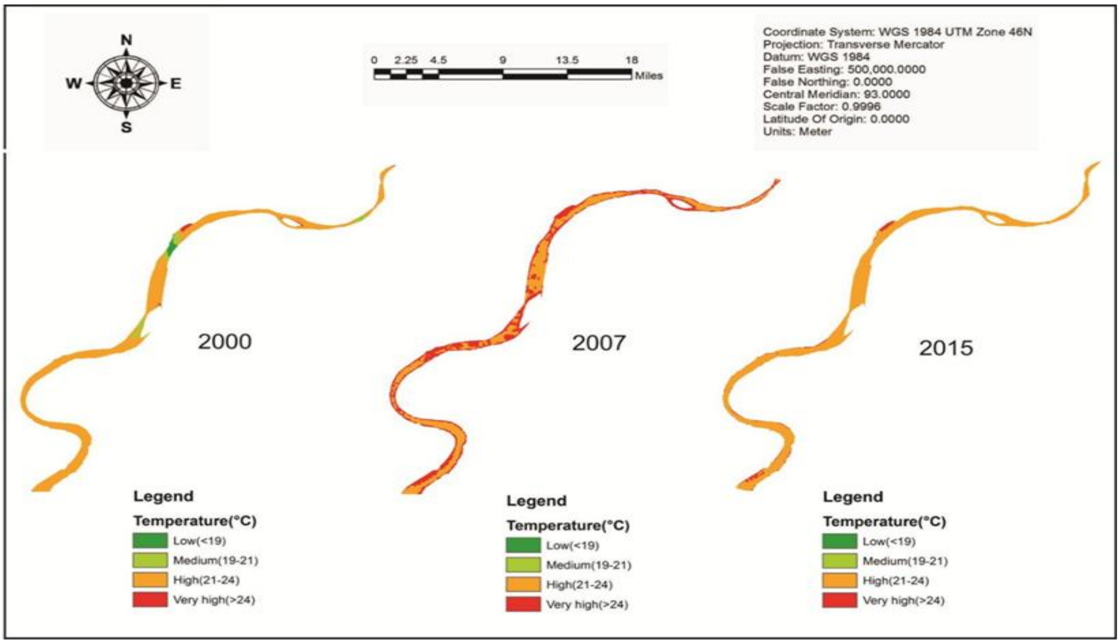

Figure 11: Temperature in March

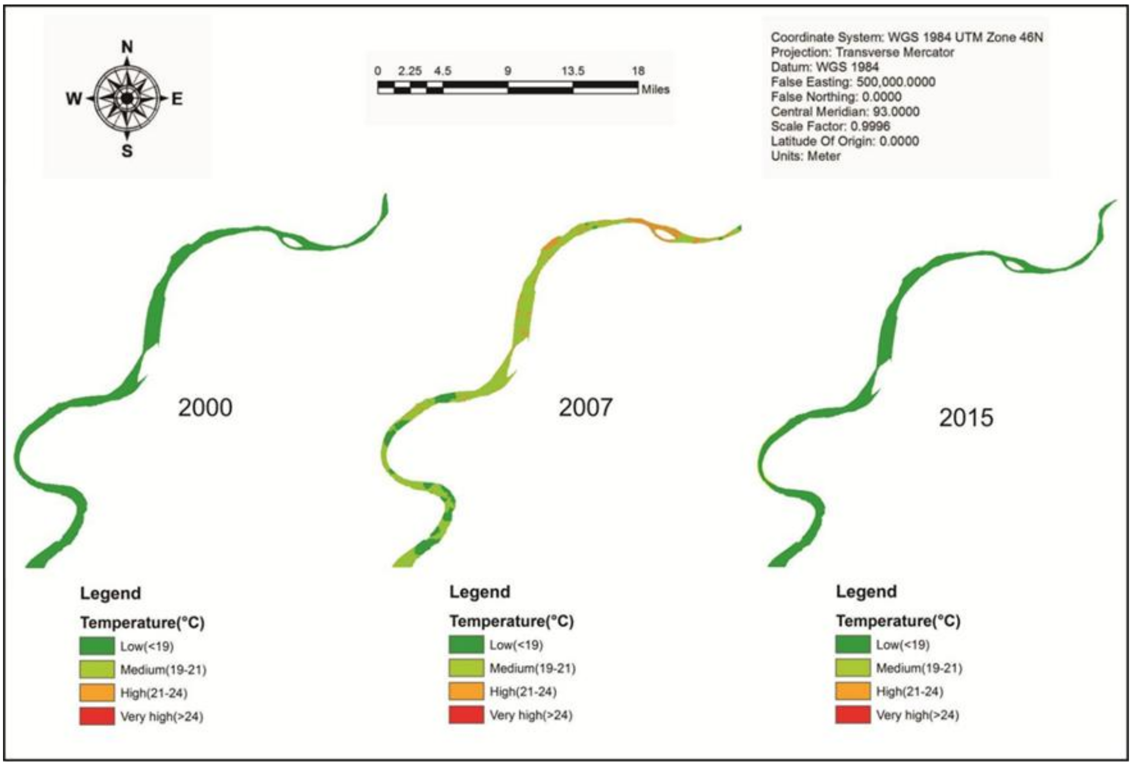

Figure 12: Temperature in July

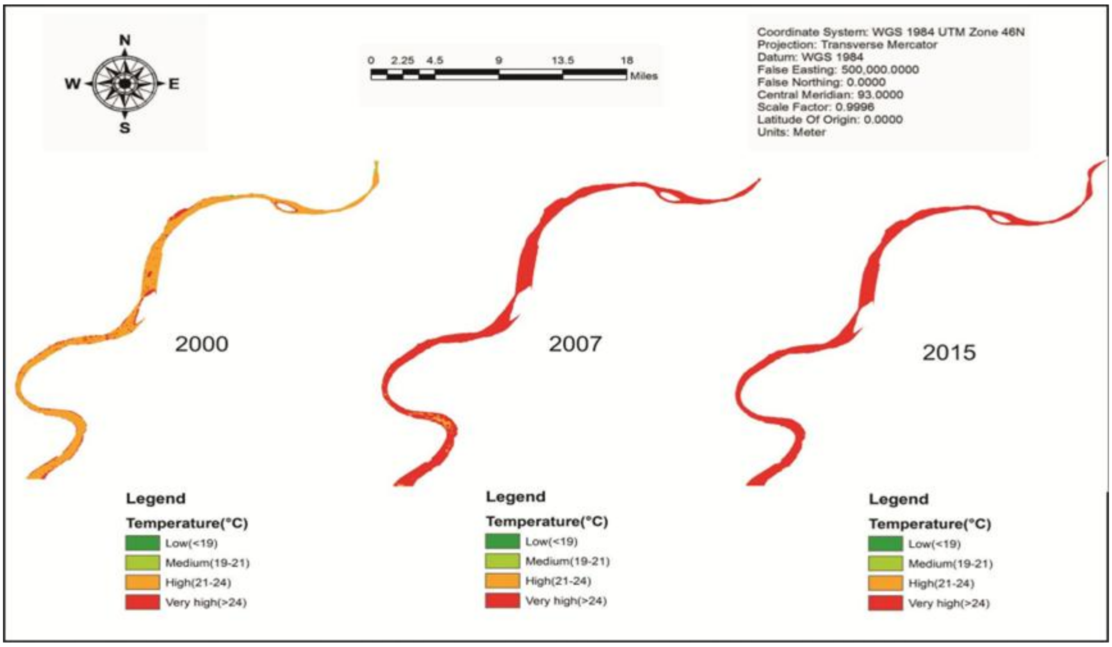

Figure 13: Temperature in November

4.4 Water Quality Assessment through Field Survey

To complement the remote sensing-based assessment, a structured field survey was conducted to gather qualitative insights from local river users. The aim of the questionnaire was to understand perceived changes in river water quality over the past 15 years, patterns of use, and associated health outcomes.

4.4.1 User Demographics and Water Usage

Survey responses revealed that household sizes were generally moderate, with 22.5% of users reporting five family members, followed by 17.5% with four members and 15% with six. Notably, 92.5% of respondents had attained primary education, while 7.5% reported completion of secondary education.

Regarding water use, 65% of respondents indicated using river water for all household purposes, including cooking, drinking, and washing. A smaller fraction reported more selective use: 20% used it exclusively for cooking, 10% for drinking, and 5% for washing. Alarmingly, 80% of users reported using the water without any prior treatment. Only 20% of the respondents stated that they boiled the water before drinking.

4.4.2 Perceptions of Water Quality

The organoleptic properties of water, such as odor and taste, serve as important proxies for perceived water quality. Approximately 42.5% of participants reported detecting a bad odor, associating it with a decline in water quality. The remaining 57.5% indicated that the water still had a normal smell.

When asked about temporal changes, 62.5% of respondents observed a deterioration in odor over the past 15 years, suggesting long-term degradation in water quality. Seasonal differences were also reported; some users noted that the water turns green during the monsoon season and blackish in winter, implying both biological and chemical alterations throughout the year.

4.4.3 Occurrence and Frequency of Waterborne Diseases

Waterborne illnesses were a central concern among the surveyed population. About 70% of respondents reported suffering from diarrhea and dysentery, with typhoid also commonly mentioned. In terms of frequency, 35% experienced such illnesses every two months, 27% reported semi-annual occurrences, and 25% indicated an approximately five-month interval.

When asked specifically about the relationship between disease occurrence and river water use, 27.5% confirmed ongoing health issues linked to water, while 35% acknowledged past issues that have become less frequent. However, 37.5% reported no occurrence of waterborne diseases. Notably, many respondents who reported disease occurrence could not conclusively attribute it to river water use, suggesting the presence of other confounding factors and limiting direct causation inference.

4.4.4 Comparative Assessment with Other Water Sources

In addition to the Karnaphuli River, local communities also rely on alternative natural and anthropogenic water sources, including a nearby waterfall, ponds, and tube wells. The waterfall, in particular, is commonly used for cooking, bathing, and drinking.

Survey results showed that 42.5% of respondents perceived noticeable physical or chemical differences between river water and other sources, while 57.5% did not report any discernible variation. This difference in perception likely reflects variations in user awareness, education, and water sensitivity thresholds.

5. Findings and Conclusion

5.1 Major Findings

This study assessed spatiotemporal variations in surface water quality in the Karnaphuli River using satellite-derived chlorophyll-a, turbidity, and temperature, supported by a field-based survey. The results were interpreted for three distinct months (March, July, and

November) across three time points (2000, 2007, and 2015), incorporating data from 15 spatially distributed observation stations.

5.1.1 Chlorophyll-a

Chlorophyll-a concentrations exhibited dynamic trends over time. During the months of March and November, values increased initially from 2000 to 2007 and subsequently declined in 2015 to levels lower than those recorded in 2000. In contrast, the month of July showed an opposite pattern—values decreased from 2000 to 2007 but rose sharply in 2015. This spike in July 2015 is likely attributable to heightened freshwater inflows during the monsoon, which can elevate nutrient loading and stimulate algal growth. Overall, the trend indicates a decline in chlorophyll-a concentrations over the study period, suggesting a gradual reduction in phytoplankton productivity.

5.1.2 Turbidity

Turbidity values remained relatively low during March and November from 2000 to 2007, followed by a notable increase in 2015, especially during the monsoon month of July. The July 2015 turbidity levels reached significantly elevated values at multiple stations, a likely consequence of increased sediment loads due to monsoonal runoff. This progressive rise indicates a deterioration in water clarity and increased sedimentation in the Karnaphuli River over the 15-year span.

5.1.3 Surface Temperature

Surface water temperatures showed a modest upward trend in March and November between 2000 and 2015. For instance, November temperatures rose from 23.56°C in 2000 to 25.28°C in 2015. However, July presented a nonlinear pattern, with a peak in 2007 followed by a drop in 2015. This anomaly may reflect climatic variability or hydrological interventions affecting mid-year thermal behavior. In general, the results point to a moderate warming trend, especially in the dry season.

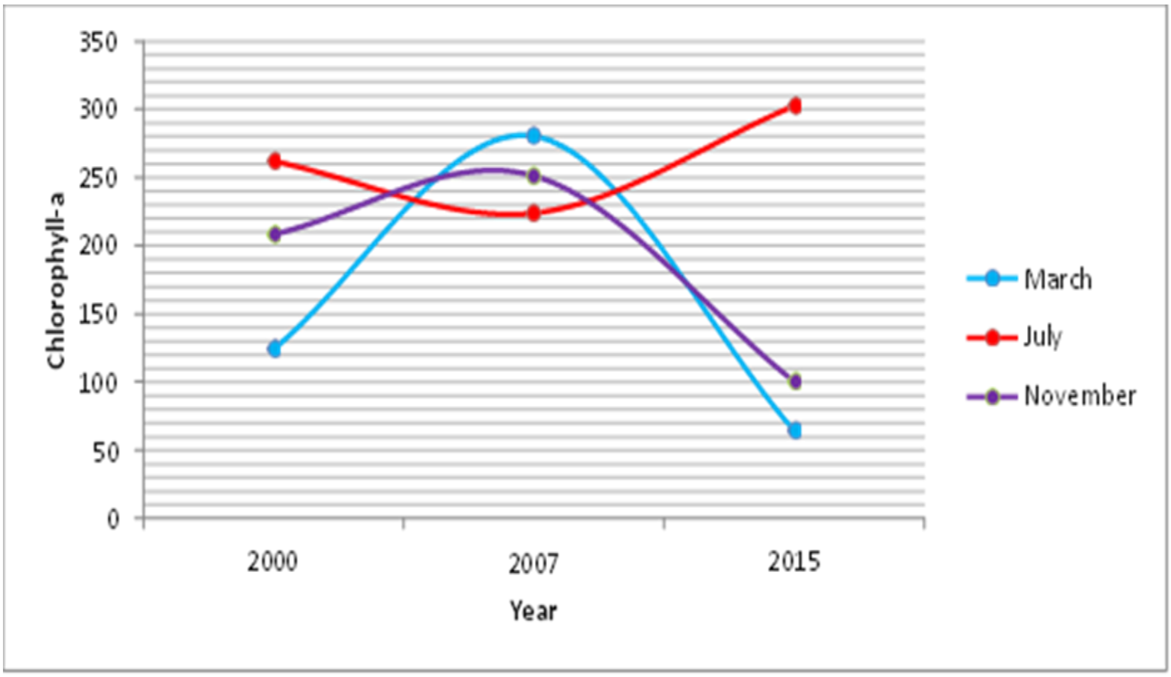

Figure 14: Average rise and fall of chlorophyll-a for different years

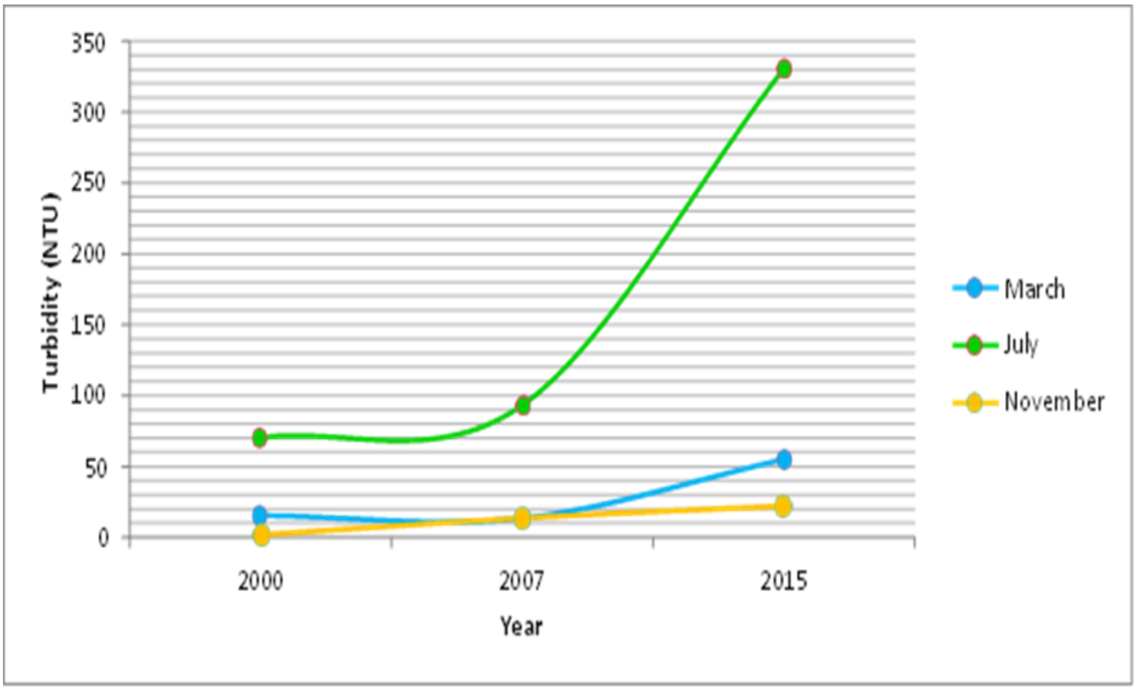

Figure 15: Average rise and fall of Turbidity for different years.

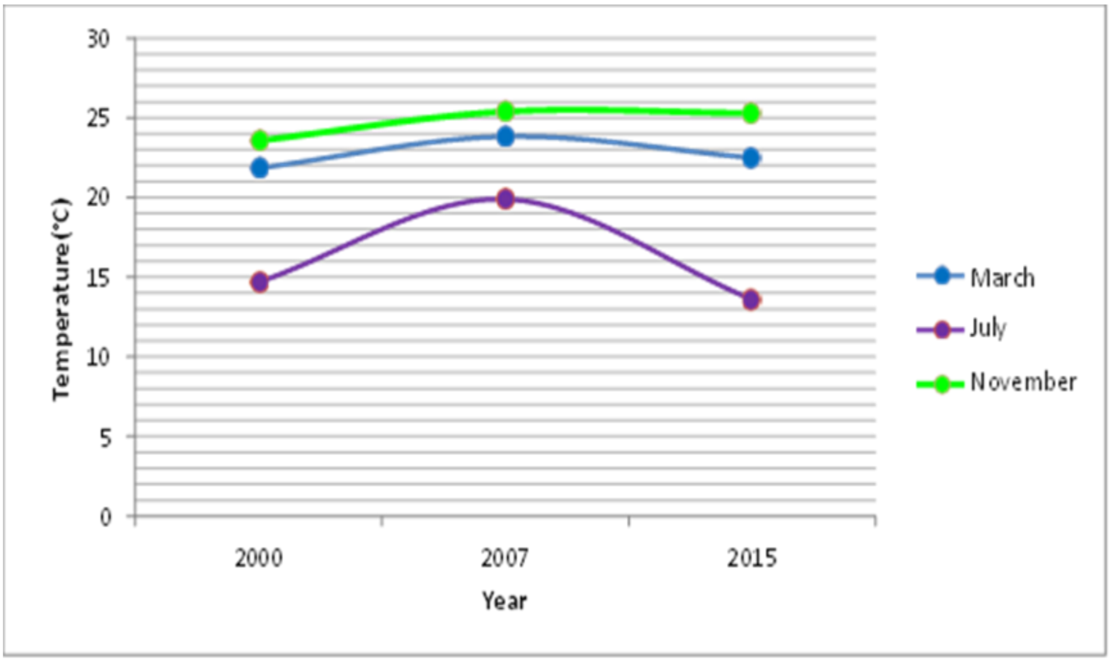

Figure 16: Average rise and fall of temperature values for different years.

5.1.4 Perceptions of Water Quality from Field Survey

The field survey highlighted growing public skepticism regarding the river's water quality. Many users reported reduced reliance on river water for domestic use and expressed a preference for alternative sources if available. The perceived deterioration in smell and color, particularly across seasons, and increased incidence of waterborne illnesses, further support the notion of declining community trust and perceived degradation in river water quality.

5.2 Conclusion

In addition to the three water quality parameters assessed in this study, the inclusion of additional indicators—such as suspended solids, salinity, alkalinity, and pathogenic presence—could have enhanced the reliability and comprehensiveness of the results. One of the key limitations of remote sensing techniques is their inability to accurately measure chemical parameters. However, remote sensing can still be effectively utilized when combined with laboratory-based measurements, allowing for the calibration of remote sensing-derived estimates through regression equations aligned with actual observed values.

Given that water quality parameters can vary considerably across different months, the constants in the regression models may require periodic adjustment to reflect seasonal variations. Laboratory analysis offers more accurate and direct measurements at specific stations, but logistical challenges make it difficult to regularly collect water samples across large and spatially diverse water bodies. In contrast, remote sensing provides a valuable, large-scale monitoring tool for rivers, lakes, and other expansive water systems, as it eliminates the need for physical access to the site, although the results may slightly deviate from actual values.

A hybrid approach that integrates laboratory measurements with remote sensing data yields the most reliable outcomes. Laboratory data are essential for calibrating and validating remote sensing-based equations, which can then be used for continuous monitoring and future projections of water quality. Despite some limitations, one of the strengths of this study is the observation of water quality across three distinct months (March, July, and November), each spaced four months apart. This temporal coverage enhances the accuracy and robustness of the findings. Overall, the results of this research provide a valuable foundation for addressing more complex challenges in water resource management and preservation at various spatial scales.

References

[1] Vignolo, A. P. (2006). Water quality assessment using remote sensing technique: Medrano Creek, Argentina. Elsevier, 429–433.

[2] Anderson, Z. Y. (2016). Estimating chlorophyll-a concentration in a freshwater lake using Landsat 8 imagery. Journal of Environmental and Earth Science, 134–140.

[3] Aydöner, E., & Yalçın, A. (2007). Water quality assessment at Ömerli Dam using remote sensing. Environmental Monitoring and Assessment.

[4] Ahmed, B., & Mahmud, H. (2013). Investigating river water quality parameters: A case study. American Journal of Civil Engineering, 84–90.

[5] Ballance, J., & Bartram, J. (1996). Water quality monitoring: A practical guide to the design and implementation of freshwater quality studies and monitoring programmes. United Nations Environment Programme and World Health Organization, Dorset, England.

[6] Biswas, M. (2013). Climate change and its impact on Bangladesh. BIP Journal, 86–95.

[7] Boney, A. D. (1988). Phytoplankton. London: Edward Arnold.

[8] Chen, S. T. (2002). Modeling the relationship between land use and surface water quality. Journal of Engineering Management, 377–393.

[9] Zhang, C., & Ma, H. (2015). Mapping chlorophyll-a concentration in Laizhou Bay using Landsat 8. IAHR World Congress Proceedings, 1.

[10] Barrett, D. C., & Eashwar, A. (2016). Automated method for monitoring water quality using Landsat imagery. MDPI, 11.

[11] Dohare, D., Deshpande, S., & Koti, S. (2014). Analysis of groundwater quality parameters: A review. Research Journal of Engineering Sciences, 26–31.

[12] Joshi, D. M., Kumar, A., & Agrawal, N. (2009). Studies of physicochemical parameters to assess the water quality of River Ganga for drinking purpose in Haridwar district. Rasayan Journal of Chemistry, 195–203.

[13] Han, L. (1997). Spectral reflectance with varying suspended sediment concentration in clear and algal-laden water. Hydrological Sciences, 701–705.

[14] Peavy, H. S., Rowe, D. R., & Tchobanoglous, G. (1985). Environmental Engineering. McGraw-Hill Book Co.

[15] Delpla, I., Jung, A., Baures, E., Clement, M., & Thomas, O. (2009). Impacts of climate change on surface water quality in relation to drinking water production. Environment International, 1225–1233.

[16] Ismail, N. U. (2010). Use of remote sensing and GIS in monitoring water quality. Journal of Sustainable Development, 228–238.

[17] Jensen, J. R. (2005). Remote Sensing of the Environment: An Earth Resource Perspective. Upper Saddle River, NJ: Prentice Hall.

[18] Anil Kumar, K. S., & Chandrasekar, P. (2015). Study on saline water intrusion into the shallow coastal aquifers of Periyar River Basin, Kerala using hydrochemical and electrical resistivity methods. Elsevier, 32–40.

[19] Kennish, M. J. (1986). Ecology of Estuaries, Vol. 2: Biological Aspects. CRC Press.

[20] Han, L., & Rundquist, D. C. (1994). The spectral responses of algal chlorophyll in water with varying levels of suspended sediments. International Journal of Remote Sensing, 3707–3718.

[21] Levin, N. (1999). Fundamentals of Remote Sensing. Trieste, Italy: IMO–International Maritime Academy.

[22] Sarwar, M. I., & Karim, A. (2010). Water quality parameters: A case study of Karnaphuli River, Chittagong. Bangladesh Journal of Scientific and Industrial Research (BCSIR), 177–181.

[23] Thirupathaia, M., & Subba Rao, C. (2012). Analysis of water quality using physico-chemical parameters in Lower Manair Reservoir of Karimnagar District, Andhra Pradesh. International Journal of Environmental Sciences, 172–180.

[24] Moore, G. K. (1980). Satellite remote sensing of water turbidity. Hydrological Sciences Journal, 407–421.

[25] Moradi, N., & Hashemi, M. (2016). Ocean color retrieval using Landsat 8 imagery in coastal Case 2 waters: Case study Oman and Persian Gulf. International Archives of Photogrammetry and Remote Sensing, 1161–1172.

[26] Shafique, N. A., Fulk, F., & Autrey, B. (2007). Hyperspectral remote sensing of water quality parameters for large rivers in the Ohio River Basin. United States Environmental Protection Agency, 216–221.

[27] Wilby, R. L., & Gleave, P. (2006). Integrated modeling of climate change impacts on water resources and quality in a lowland catchment: River Kennet, UK. Elsevier, 204–220.

[28] Gorde, S. P., & Jadhav, M. V. (2013). Assessment of water quality parameters: A review. International Journal of Engineering Research and Applications, 6.

[29] Gorde, S. P., & Jadhav, M. V. (2013). Assessment of water quality parameters: A review. International Journal of Engineering Research and Applications, 2029–2035.

[30] Bauni, V., & Schaeffer, F. (2015). Ecosystem loss assessment following hydroelectric dam flooding: The case of Yacyretá, Argentina. Elsevier, 50–60.

[31] Venkateswarlu, G. (2003). Analytical study of effects of water quality parameters using remote sensing and GIS under Hyderabad Urban Area Zone-V. International Journal of Research in Engineering & Technology, 308–315.

Citation: Kaiser Mostafiz, Shishir Kumar Das, Mohammad Noor Uddin. (2025). Assessing Spatiotemporal Water Quality Changes in the Karnaphuli River in Bangladesh Using Remote Sensing Techniques. International Journal of Civil Engineering and Technology (IJCIET), 16(3), 13-42.

Abstract Link: https://iaeme.com/Home/article_id/IJCIET_16_03_002

Article Link:
https://iaeme.com/MasterAdmin/Journal_uploads/IJCIET/VOLUME_16_ISSUE_3/IJCIET_16_03_002.pdf

✉ **editor@iaeme.com**